

Electromigration Performance of Pb-free Solder Joints in Terms of Solder Composition and Joining Path

Sun-Kyoung Seo, Sung K. Kang, Moon Gi Cho, and Hyuck Mo Lee

The electromigration (EM) performance of Pb-free solder joints is investigated in terms of solder composition (Sn-0.5Cu vs. Sn-1.8Ag) and joining path to Cu vs. Ni(P) under bump metallization (UBM). In the double-sided joints of Ni(P)/solder/Cu, the microstructure of solder joints and the interfacial intermetallic compound (IMC) layers are significantly affected by solder composition and joining path. The as-reflowed microstructure of Sn-0.5Cu joints consists of small columnar grains with thin IMC layers at both UBM interfaces, independent of the joining path, while Sn-1.8Ag joints have a few large grains of low-angle grain boundaries with thick IMC layers when joined first to Ni(P) UBM, but a few 60° twins with thin IMC layers when joined first to Cu UBM. The EM stressing under high current densities at 150°C reveals that Sn-1.8Ag joints have a superior lifetime compared to Sn-0.5Cu joints. In addition, the EM lifetime of Sn-1.8Ag joints reflowed first on Ni(P) UBM is the longest among four groups of the solder joints examined.

INTRODUCTION

The requirements of a smaller form factor and higher performance in microelectronic products continuously increase the current densities both in the Cu or Al thin film lines and at flip-chip solder joints. Accordingly, concern about electromigration (EM) performance of flip-chip interconnections has become more serious in recent years. The increased current density of the EM performance of solder joints would cause higher driving forces for the diffusion of all the materials in its path and an increase in Joule heating.¹⁻⁴ The fast diffusion of materials and high joule heating by the current crowding were

commonly reported to lead to the failures of solder joints.¹⁻⁴ Therefore, EM stressing has become one of the most important reliability tests, especially for Pb-free, flip-chip solder joints.

Most Pb-free solders consisting of more than 90% Sn and a few alloying elements such as Ag, Cu, and Ni are

commonly added to Sn to improve various physical or mechanical properties of Pb-free solders.⁵⁻⁸ These elements are known to be the fast diffusers in Sn matrix by moving through the interstitial sites of Sn matrix.⁹⁻¹² Especially, the diffusivities of Cu and Ni are two to five orders faster than Ag and four to nine orders faster than Sn self-diffusivity at 150°C.⁹⁻¹² In addition, since β -Sn has anisotropic properties, the consumption of under bump metallization (UBM) is varied according to the crystal orientation of β -Sn in solder under current stressing.¹³ Namely, the compositions and β -Sn grain orientation of Pb-free solders are found to be important factors in determining EM failure of Sn-rich solder joints.

In the previous studies,^{14,15} the β -Sn grain orientations of Sn-0.5Cu and Sn-1.8Ag were also found to be very different depending the choice of Cu vs. Ni(P) UBM. When Sn-0.5Cu solder balls were joined to Cu UBM, the dissolution of Cu from UBM led to form many columnar grains having near $\langle 110 \rangle$ crystal direction in Sn-0.5Cu/Cu joint, while low-angle large grains were formed to have near $\langle 001 \rangle$ or $\langle 100 \rangle$ orientations in Sn-1.8Ag/Cu joint. In contrast, when Sn-0.5Cu solder balls were jointed to Ni(P) UBM, the dissolution of Ni led to form beach-ball shaped cyclic twins having various crystal directions in Sn-0.5Cu/Ni(P) joint, while low-angle large grains were formed in Sn-1.8Ag/Ni(P) joint having $\langle 111 \rangle$ crystal directions. In double-sided joints, Ni(P)/solder/Cu, the dissolution of both Cu and Ni can affect the microstructure of solder joints. When assembling a double-sided joint, the joining path (first to Cu or Ni(P) UBM) could be a critical factor to determine their microstructure. This study investigated the effects of joining path

How would you...

...describe the overall significance of this paper?

Electromigration (EM) performance is a key reliability issue of Pb-free solder joints used in high performance electronics. This paper reports that solder composition and joining path to Cu or Ni(P) significantly affect the grain orientation of Sn and the intermetallic thickness, which strongly influence the EM lifetime of Sn-rich solder joints.

...describe this work to a materials science and engineering professional with no experience in your technical specialty?

The anisotropic properties of Sn crystal critically affect the reliability of Pb-free solders, such as in electromigration or thermal fatigue. This paper reports that Sn-rich solder composition and joining path to under bump metallization significantly change Sn grain orientation and intermetallic compound thickness, affecting EM lifetime of Pb-free solder joints.

...describe this work to a layperson?

The environmental issue of replacing Pb-containing solders with Pb-free solders in microelectronics is discussed. This paper reports on the one key reliability issue of Pb-free solders—electromigration performance. The solder composition and interfacial reactions of Sn-rich solders are found to significantly affect the EM lifetime of Pb-free solder joints.

on their microstructure with two different solder compositions, Sn-0.5Cu vs. Sn-1.8Ag. Also, the electromigration performance of Pb-free solder joints is investigated in terms of solder composition and joining path to Cu or Ni(P) UBM. The corresponding EM lifetime and their failure mechanisms are explained based on solidification microstructure, Sn grain orientation, and interfacial reactions.

See the sidebar for experimental procedures.

RESULTS AND DISCUSSION

The Effects of Joining Path on the Microstructure in Double-sided Solder Joints

To study the effects of the joining path, the microstructure of as-reflowed solder joints were investigated in terms of their β -Sn grain orientation, interfacial intermetallic compound (IMC) formation, and the composition of solder matrix. Figure 1 shows the typical electron backscatter diffraction (EBSD) images and inverse pole figures of four different joints as-reflowed over more than 30 samples; (Ni)Sn-0.5Cu, (Cu)Sn-0.5Cu, (Ni)Sn-1.8Ag, and (Cu)Sn-1.8Ag. (Ni)Sn-0.5Cu and (Cu)Sn-0.5Cu joints have similar β -Sn grain orientation, small columnar grains with the major $\langle 110 \rangle$ crystal direction perpendicular to the substrate. This crystal orientation, $\langle 110 \rangle$, is well known for Sn dendrite growth in bulk solidification.¹⁶ In addition, a similar high-angle solidification boundary in (Ni)Sn-0.5Cu reported previously¹⁷ was also observed in (Cu)Sn-0.5Cu joints. From the EBSD analysis, it is found that the β -Sn grain orientation in Sn-0.5Cu joints was not affected by the joining path. However, it is noted that for Sn-1.8Ag joints the β -Sn grain orientation varies according to the joining path. As shown in Figure 1c and d, low-angle large grains having $\langle 111 \rangle$ or $\langle 110 \rangle$ or $\langle 101 \rangle$ crystal directions are observed in (Ni)Sn-1.8Ag joints, while three or four 60° cyclic twins having near $\langle 111 \rangle$ and $\langle 001 \rangle$ crystal directions are frequently observed in (Cu)Sn-1.8Ag joints.

Figure 2 shows the typical IMC layers formed at the interfaces of solder/Ni(P) UBM (top) and solder/Cu UBM (bottom). In all interfaces, $(\text{Cu}, \text{Ni})_6\text{Sn}_5$ phase is formed. At the Ni UBM inter-

EXPERIMENTAL PROCEDURES

To form a double-sided joint of Ni(P)/solder/Cu, two kinds of printed circuit boards (PCB) were designed and manufactured as shown in Figure A; PCB1 (large) and PCB2 (small). Cu OSP is the surface finish of PCB1, while Ni(P)/Au is the surface finish of PCB2. The size of open pad is $300 \mu\text{m}$ in diameter and the pitch size is $800 \mu\text{m}$. Solder balls of Sn-0.5Cu and Sn-1.8Ag (wt.%) with $380 \mu\text{m}$ in diameter were joined to Cu UBM of PCB1 and Ni(P) UBM of PCB1 by reflowing them in a 250°C oven for 2 min.

To investigate the effects of joining path on the microstructure and electromigration (EM) lifetime, double-sided joints were formed through two paths of the reflow process as shown in Figure B. One path is that a solder ball is first joined to Ni(P) UBM (on PCB2), and then to Cu UBM. Another path is that a solder ball is first joined to Cu UBM (on PCB1), and then to Ni(P) UBM. Sample identification was made by referring the first joining path. Sn-0.5Cu joints reflowed on Ni(P) UBM first and then reflowed on Cu UBM are named as “(Ni)Sn-0.5Cu.” And, Sn-0.5Cu joints reflowed on Cu UBM first and then reflowed on Ni(P) UBM are named as “(Cu)Sn-0.5Cu.” Sn-1.8Ag joints also are named in the same way as “(Ni)Sn-1.8Ag” and “(Cu)Sn-1.8Ag.”

During electromigration stressing, the electric current has been passed through only two joints in one module sample, as shown in Figure C. The rest of the joints in the same row were used as the reference joints with no current stressing, only with thermal exposure. A constant current of 10A ($14,150 \text{ A/cm}^2$) or 7A ($9,900 \text{ A/cm}^2$) was applied to the two solder joints under test. Samples were placed in a silicone oil bath on the hotplate to maintain a uniform and stable temperature. The temperature measured using a thermocouple between the tested solder joints was maintained to be at 150°C during EM test. The change in resistance was measured and the data were collected in computer in situ.

The solder joints were cross-sectioned, fine-polished and examined with electron backscatter diffraction (EBSD) to obtain the information on grain size and crystal orientation of β -Sn. The major crystal direction of β -Sn to the substrates was analyzed with regard to the rotation direction, $[001]$. The microstructure of interfacial intermetallic compound layers and solder inside was also examined using scanning electron microscopy (SEM) and optical microscopy (OM). The electron probe micro-analysis (EPMA) was used for quantitative composition analyses of solder joints.

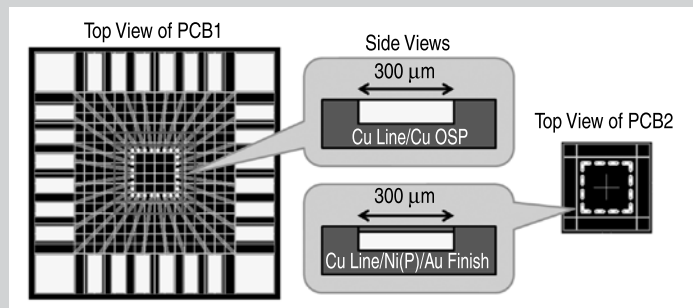


Figure A. The PCB design for EM test of solder joints.

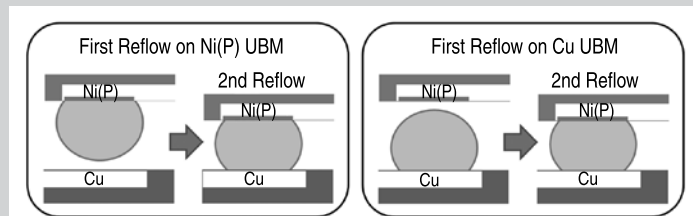


Figure B. Two joining paths for the double-sided joints, Ni(P)/solder/Cu.

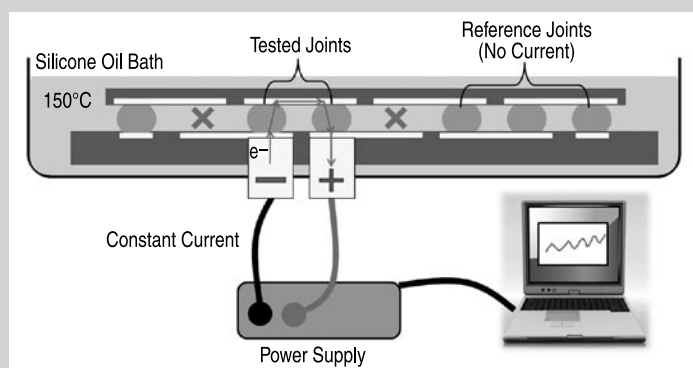


Figure C. The setup of EM test of solder joints.

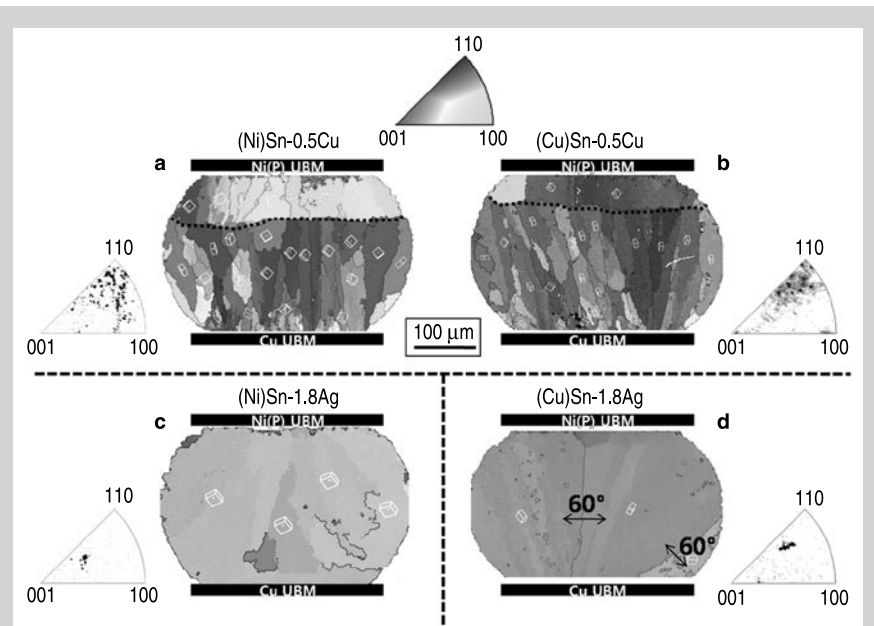


Figure 1. EBSD images and inverse pole figures of (a) (Ni)Sn-0.5Cu, (b) (Cu)Sn-0.5Cu, (c) (Ni)Sn-1.8Ag, and (d) (Cu)Sn-1.8Ag solder joints as-reflowed.

face in (Ni)Sn-1.8Ag, $(\text{Ni,Cu})_3\text{Sn}_4$ layer is first formed during the first reflow, and then $(\text{Cu,Ni})_6\text{Sn}_5$ layer is formed on top of the $(\text{Ni,Cu})_3\text{Sn}_4$ layer during the second reflow. The interfacial IMCs in (Ni)Sn-1.8Ag joints of both UBM interfaces are much thicker than in other solder joints, as shown in Figure 2. The thick IMC layer at the Cu UBM consists of two layers, $(\text{Cu}_{0.93}\text{Ni}_{0.07})_6\text{Sn}_5$ and $(\text{Cu}_{0.86}\text{Ni}_{0.14})_6\text{Sn}_5$ differentiated by the

amount of Ni substitution in (Ni)Sn-1.8Ag joints. This compositional analysis of $(\text{Cu,Ni})_6\text{Sn}_5$ IMCs consisting of two layers at the Sn-1.8Ag/Cu interface is similar to the previous result reported for the Sn-3.5Ag solder/Cu interface.¹⁷ While Sn-0.5Cu and Sn-1.8Ag joints reflowed first on Ni(P) UBM have different interfacial IMC layers in terms of their composition and thickness, Sn-0.5Cu and Sn-1.8Ag joints reflowed

first on Cu UBM have the same interfacial IMC layers, $(\text{Cu}_{0.93}\text{Ni}_{0.07})_6\text{Sn}_5$ at the Ni(P) UBM and $(\text{Cu}_{0.99}\text{Ni}_{0.01})_6\text{Sn}_5$ at the Cu UBM.

The interfacial reactions with Cu and Ni(P) UBMs can change the composition in solder and significantly affect the microstructure.¹⁴ Table I shows the result of EPMA analysis. The analysis was conducted at the central area of about 200 μm in diameter. The compositions of Cu and Ni in solder are affected by the joining path. When solders are joined first on Ni(P) UBM, Ni content in solder is somewhat higher than in solders joined first on Cu UBM in both Sn-0.5Cu and Sn-1.8Ag joints. However, Cu content in solder is affected by both the initial solder composition and joining path. Although Cu contents in (Cu)Sn-0.5Cu and (Ni)Sn-0.5Cu joints are similar to each other, the Cu content in (Cu)Sn-1.8Ag joints is about 0.3 wt.% higher than in (Ni)Sn-1.8Ag joints. Since the thicker IMC layers are formed in (Ni)Sn-1.8Ag, more Cu atoms must be dissolved from Cu UBM and consumed to form the thick IMC layers at both interfaces. This might lead to a lower Cu content at the central area in (Ni)Sn-1.8Ag than in (Cu)Sn-1.8Ag. The difference of Ni content in different solders is too small, below 0.1 wt.%, which is in the range of detection

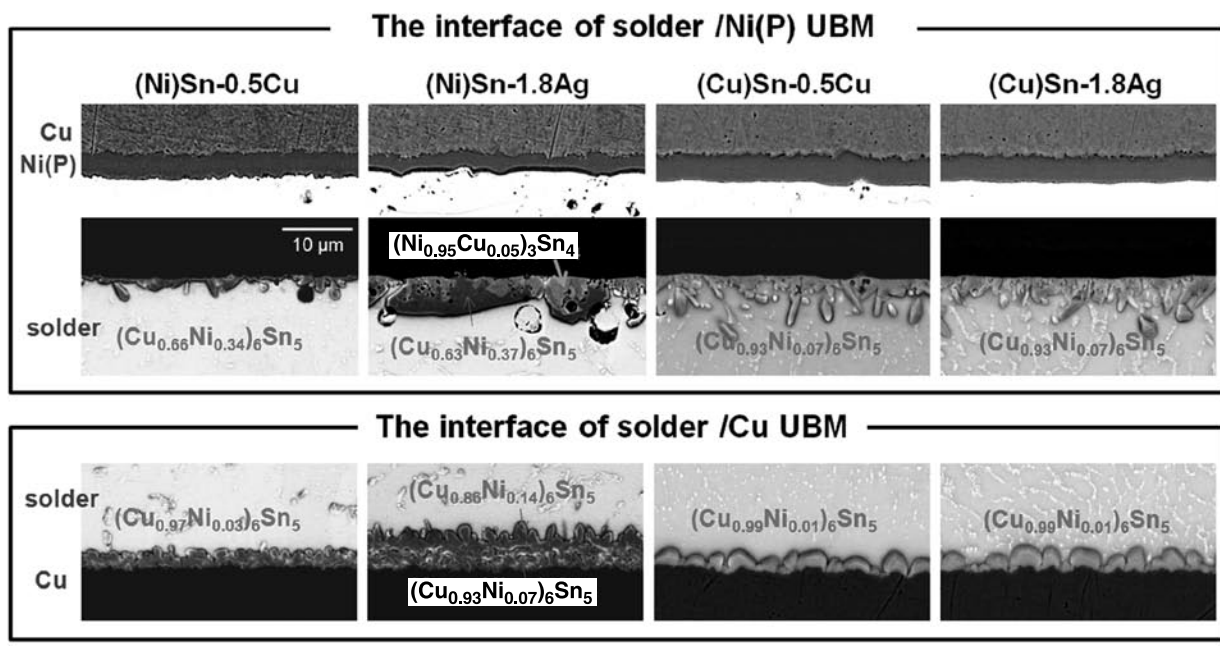


Figure 2. IMC layers at the interfaces of solder/Ni(P) UBM and solder/Cu UBM in (Ni)Sn-0.5Cu, (Cu)Sn-0.5Cu, (Ni)Sn-1.8Ag, and (Cu)Sn-1.8Ag solder joints as-reflowed.

Table I. The Result of EPMA Composition Analysis in the Area with 200 μm in Diameter

Solder Joint	Composition (wt.%)				
	Ag	Cu	Ni	Sn	Total
(Ni)Sn-0.5Cu	—	1.22	0.08	Balance	100
(Cu)Sn-0.5Cu	—	1.18	0.01	Balance	100
(Ni)Sn-1.8Ag	1.78	0.53	0.08	Balance	100
(Cu)Sn-1.8Ag	2.08	0.84	0.02	Balance	1,000

limit. However, the difference of 0.3 wt.% Cu is large enough to change the microstructure. The 0.3 wt.% higher Cu content in (Cu)Sn-1.8Ag joints can significantly affect the β -Sn grain orientation and yield higher propensity of 60° cyclic twins compared to (Ni)Sn-1.8Ag joints.

Electromigration Lifetime of Solder Joints

From the microstructure analysis of solder joints in the previous section, it is found that the joining path to Cu vs. Ni(P) UBM can produce large variations in the microstructure, thickness of IMC layers, Cu solute content, and propensity of cyclic twins, especially in Sn-Ag solder joints. In order to further investigate how the joining path and the solder composition (Sn-0.5Cu vs. Sn-1.8Ag) affect EM reliability of solder joints, double-sided solder joint samples are tested under a constant current at an elevated temperature of 150°C. When 7A and 10A current are applied to solder joints, the current density at the joint is estimated to be 9,900 A/cm² and 14,150

A/cm², respectively. Figure 3 exhibits the changes of resistance (Ω) with time with four groups of solder joints under two constant current densities. The abrupt increase of resistance is regarded as an open failure of a solder joint as marked in Figure 3 for each joint. Table II summarizes the mean time to failure (MTTF) of four joints under 10A and 7A. The 40% increase in current density results in the significant reduction in MTTF. The MTTF of (Cu)Sn-0.5Cu and (Ni)Sn-0.5Cu joints under 10k A/cm² is 3~4 times longer than under 14k A/cm². Also, the MTTF of (Cu)Sn-1.8Ag and (Ni)Sn-1.8Ag joints under 10k A/cm² is about 8 times longer than under 14k A/cm².

The important information from Table II is that the MTTF of solder joints strongly depends on the solder composition as well as the joining path. The ranking of the four solder joints in terms of the EM lifetime, from the worst to best, is found under both current densities,

$$(Cu)Sn-0.5Cu \approx (Ni)Sn-0.5Cu < (Cu)Sn-1.8Ag \ll (Ni)Sn-1.8Ag.$$

Table II. EM Lifetime of Solder Joints under 14k A/cm² and 9.9k A/cm²

Applied Current (A)	Current Density (A/cm ²)	Solder Joint	MTTF (h)
7	9.9×10^3	(Ni)Sn-0.5Cu	74
		(Cu)Sn-0.5Cu	50
		(Ni)Sn-1.8Ag	646
		(Cu)Sn-1.8Ag	229
10	14×10^3	(Ni)Sn-0.5Cu	18
		(Cu)Sn-0.5Cu	16
		(Ni)Sn-1.8Ag	78
		(Cu)Sn-1.8Ag	28

The lifetime of Sn-0.5Cu solder joints is generally much shorter than Sn-1.8Ag solder joints, as previously reported.¹³ In addition, while the lifetime of Sn-0.5Cu joints does not depend on the joining path, the lifetime of Sn-1.8Ag joint strongly depends on the joining path. The MTTF of (Ni)Sn-1.8Ag joints is about three times longer that of (Cu)Sn-1.8Ag joints under both 10k A/cm² and 14k A/cm² current stressing.

In order to understand the critical factors determining the EM lifetime of solder joints, the microstructure of the failed joints under 14k A/cm² are examined on their cross sections as shown in Figure 4. In all samples, severe dissolution of Cu lines on PCB (top) and extensive formation of Cu₆Sn₅ phase in the solder joints are observed in the right side joints, where electrons entering at the upper left corner of the joint and passing top to bottom. The microstruc-

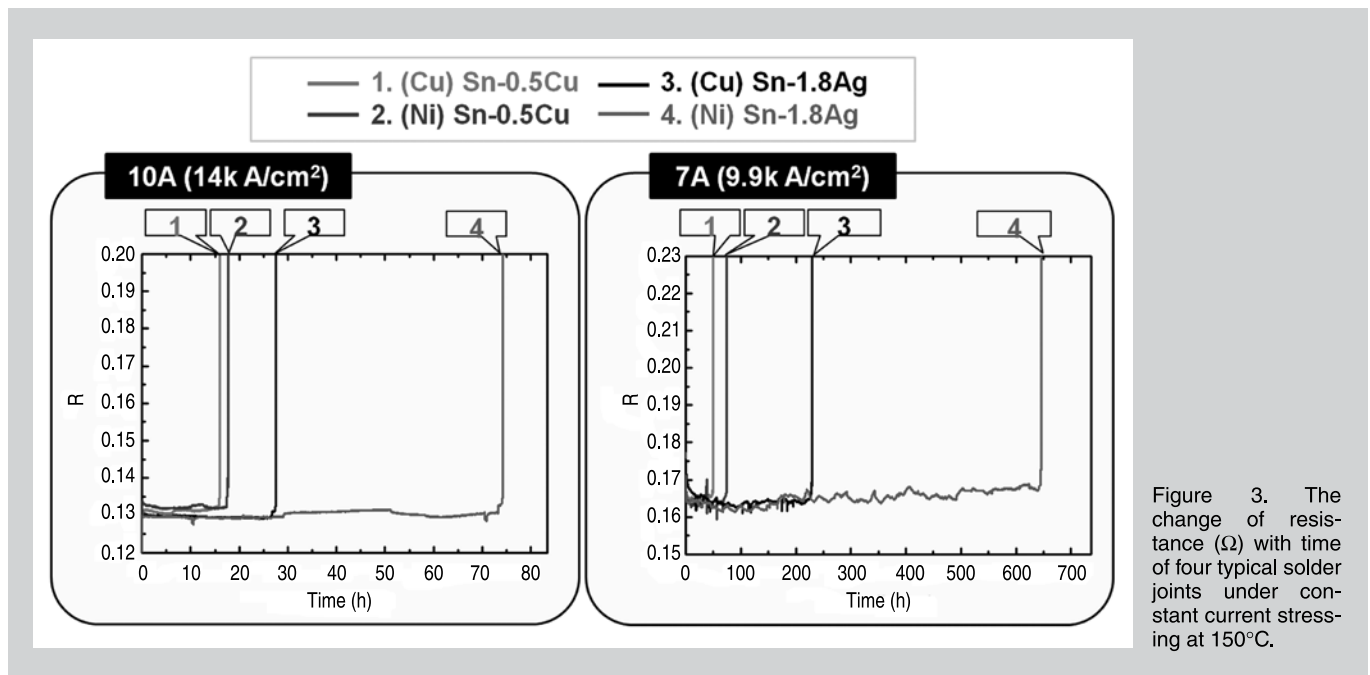


Figure 3. The change of resistance (Ω) with time of four typical solder joints under constant current stressing at 150°C.

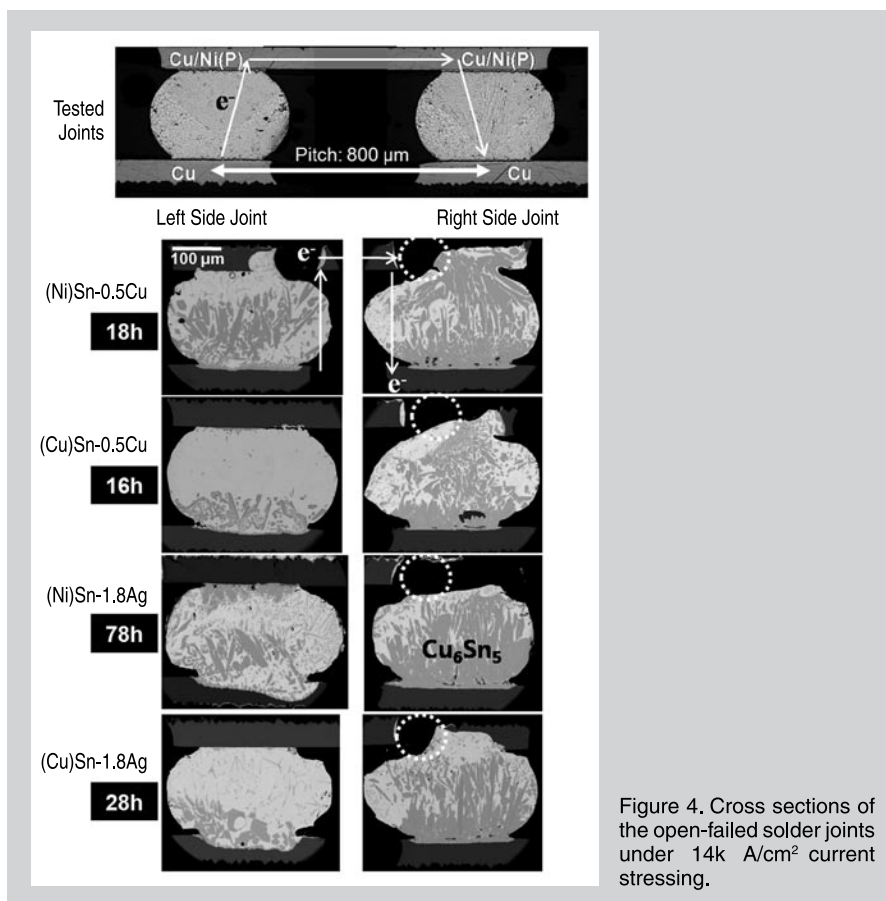


Figure 4. Cross sections of the open-failed solder joints under 14k A/cm² current stressing.

ture of the failed joints under 10k A/cm² was similar to that under 14k A/cm². At the solder/UBM interfaces of the right-side joints, current crowding and high joule heating are observed, where severe Cu dissolution is noted. In other studies, two-dimensional simulation of current distribution in a solder joint and infrared image of the cross-sectioned joint demonstrated the local higher current density and accompanying joule heating at the interfaces of solder joints.^{1,4} Actually, in this study, the current density at the Cu line is estimated to be 34,188 A/cm², which is more than two times higher than the current density at the solder/UBM interface, 14,147 A/cm². At the upper-left corner in the right side joint, local joule heating can cause the melting of solder and may lead to an open electrical failure of the joint. However, by analyzing the final microstructure of EM failed joints, it is difficult to catch the critical factors determining the different EM performance of different solder joints.

Consequently, the microstructure examination of solder joints in the intermediate stage of EM stressing before open failure is needed to find important factors determining the different EM

lifetime, as discussed in the following section.

Microstructure of Solder Joints after 10 h under 14k A/cm² Current Stressing

To compare their microstructural changes during the intermediate stage of EM stressing, four groups of solder joints are tested for a duration of 10 h under 14k A/cm² at 150°C. Figure 5 shows the representative cross-sectioned optical images, EBSD images, and inverse pole figures from the 10 h EM tested solder joints. The microstructure of Sn-0.5Cu joints is significantly different from Sn-1.8Ag joints. Especially, the consumption of Cu UBM at the cathode side of the left-side joint is larger in Sn-0.5Cu joints than in Sn-1.8Ag joints. And, the consumption of Cu UBM is larger in (Cu)Sn-1.8Ag joints than in (Ni)Sn-1.8Ag joint. The large consumption of Cu UBM has led to form the large amount of Cu₆Sn₅ phase inside the solder joint. Comparing to the reference joints under no current stressing, the coarsening of Cu₆Sn₅ in the EM tested joints is significant. In (Ni)Sn-0.5Cu and (Cu)Sn-0.5Cu joints where IMC particles are dominantly Cu₆Sn₅, no in-

termetallic particles are observed in the solder matrix after 10 h EM stressing, except the coarsened large Cu₆Sn₅ along the grain boundaries of β-Sn as shown in Figure 6e and f. In (Ni)Sn-1.8Ag and (Cu)Sn-1.8Ag joints of Figure 6g and h, coarsened Ag₃Sn particles remain in the solder matrix after 10 h EM stressing, while most coarsened Cu₆Sn₅ particles are found along 60° twin boundaries or low-angle grain boundaries. In addition, the coarsening rate of Ag₃Sn is much smaller than Cu₆Sn₅ during the EM stressing. This is one of reasons why Sn-1.8Ag joints have a longer EM lifetime compared to Sn-0.5Cu joints under the same EM test conditions.

In both (Ni)Sn-0.5Cu and (Cu)Sn-0.5Cu joints, small columnar grains with the major <110> crystal direction in as-reflowed joints (Figure 1) have significantly coarsened with various crystal orientations after 10 h EM stressing. And, many coarsened Cu₆Sn₅ particles are found along the grain boundaries of various high-angle orientations (44–95°). During aging at 150°C for 250 h without current stressing, it was found that the small columnar grains of Sn-0.5Cu joints coarsened maintaining the <110> crystal direction as the major crystal direction perpendicular to the substrate.¹⁷ However, under current stressing, the β-Sn grain orientation has changed to various directions with high misorientation angles during the grain coarsening. Since high-angle grain boundaries provide a fast diffusion path for Cu atoms, many coarsened Cu₆Sn₅ particles are observed along these boundaries after 10 h EM as shown in Figure 5a and b.

Contrary to Sn-0.5Cu joints, the change of β-Sn grain orientation in Sn-1.8Ag joints under current stressing is very little. Low-angle large grains and three or four 60° cyclic twins observed commonly in as-reflowed (Ni)Sn-1.8Ag and (Cu)Sn-1.8Ag joints, respectively, are maintained after 10 h EM stressing. Under current stressing, Cu atoms can dissolve from Cu UBM and Cu-Sn IMC layer at the cathode into solder through low-angle grain boundaries or Sn lattice. The migration of Cu atoms through low-angle grain boundaries or Sn lattice in Sn-1.8Ag joints is expected to be much slower than through high-angle grain boundaries, such as in Sn-0.5Cu

joints.

It is interesting to note that the 60° twin boundaries observed in the (Cu)Sn-1.8Ag joint, Figure 5d is fully occupied with coarsened Cu_6Sn_5 particles. This means that 60° twin boundary can also provide a fast diffusion path for Cu atoms in addition to high-angle grain boundaries. In (Cu)Sn-1.8Ag as-reflowed joints, it is observed that the tendency of having 60° cyclic-twins is higher than the (Ni)Sn-1.8Ag joints. This seems to ex-

plain why (Cu)Sn-1.8Ag joints have a shorter EM lifetime than (Ni)Sn-1.8Ag joints. Again, it is confirmed that the joining path to Cu or Ni(P) UBM has a significant bearing on their EM performance of the corresponding solder joints.

Figure 7 exhibits the interfacial IMC layers of the solder joints both after 10 h EM stressing and without current stressing (reference joints). For the EM stressed joints, the cross sections of both

the left and right side joints are shown for each group. By comparing the thickness of IMC layers at two UBM interfaces, the migration speed of Cu atoms in each solder joint would be estimated. In both (Ni)Sn-0.5Cu and (Cu)Sn-0.5Cu, the change of IMC thickness is obvious in EM tested joints; Cu_6Sn_5 layers at the Cu UBM of the left-side joint and at the Ni(P) UBM of the right-side joint become thinner, while Cu_6Sn_5 layers at other interfaces become thicker.

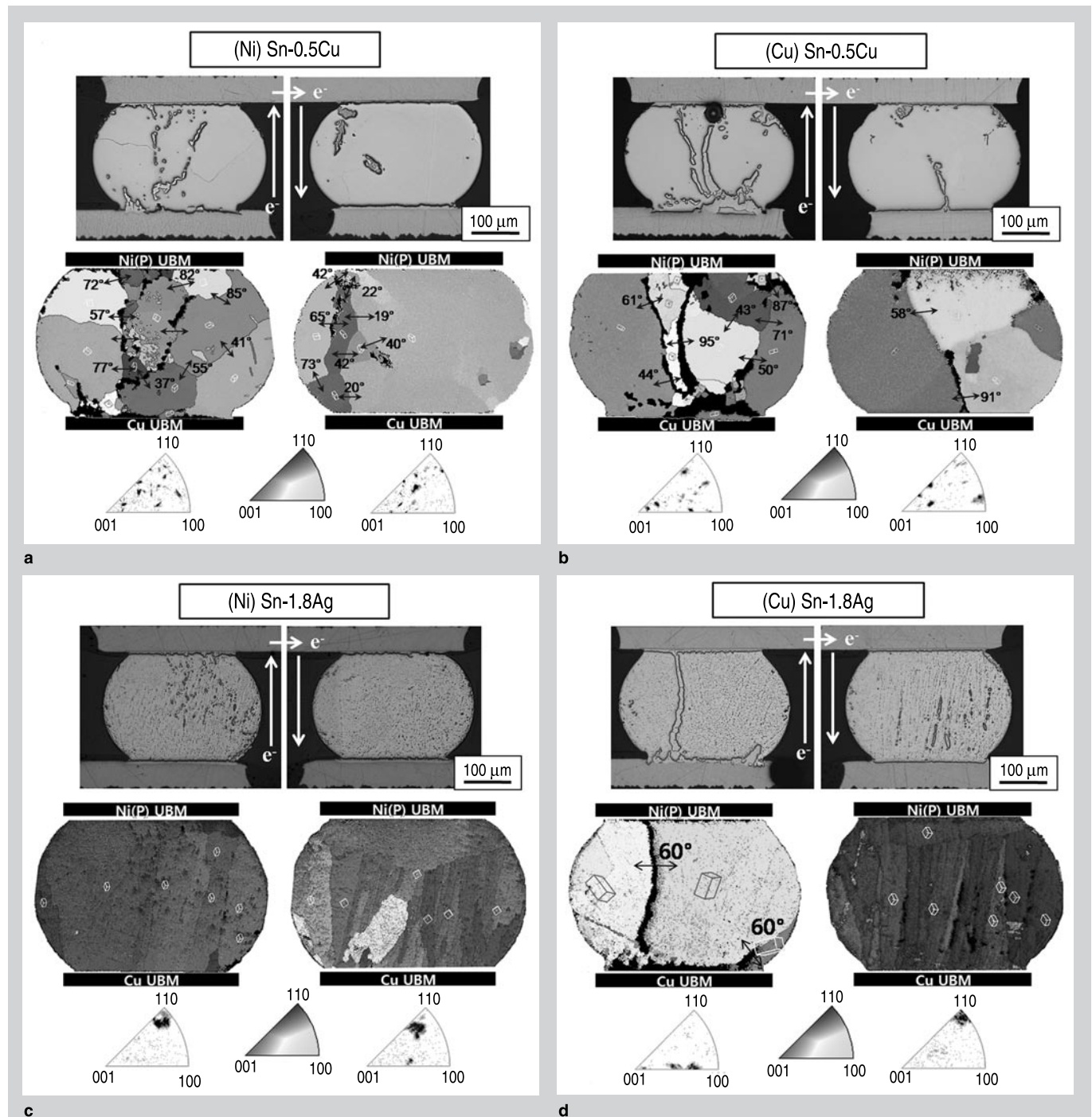


Figure 5. Optical images, EBSD images, and inverse pole figures of (a) (Ni)Sn-0.5Cu, (b) (Cu)Sn-0.5Cu, (c) (Ni)Sn-1.8Ag, and (d) (Cu)Sn-1.8Ag solder joints after EM test under 14 k A/cm^2 , for 10 h.

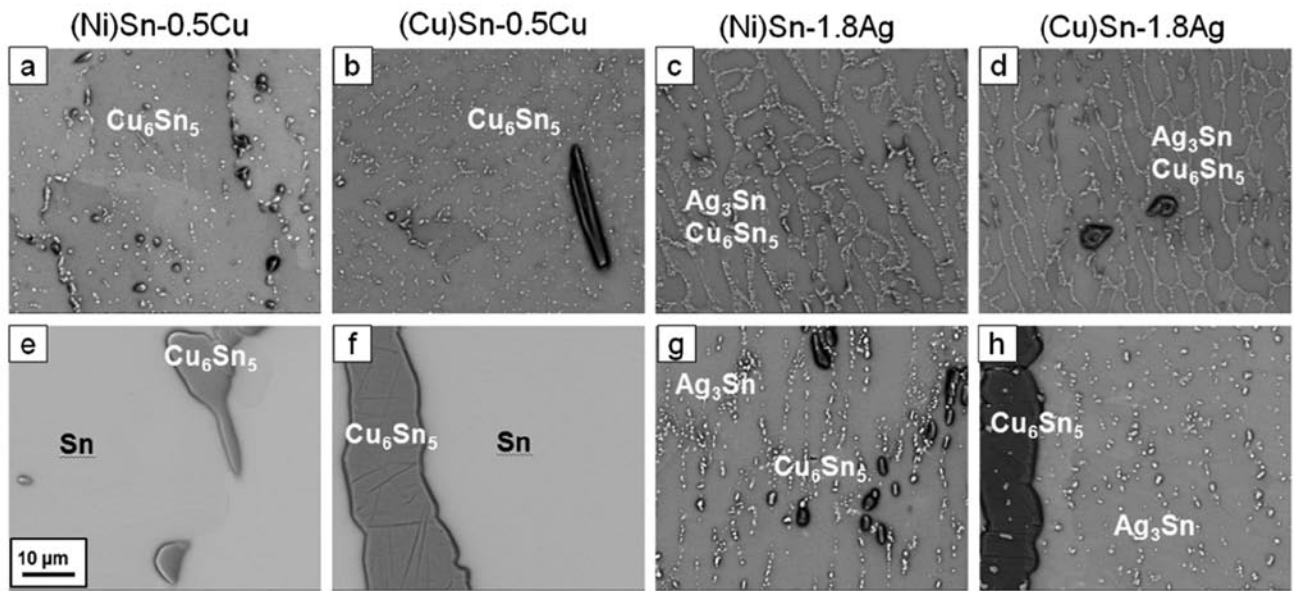


Figure 6. SEM images of inside solder in four solder joints under no current stressing (a–d) and under 14k A/cm² constant current stressing for 10 h (e–h).

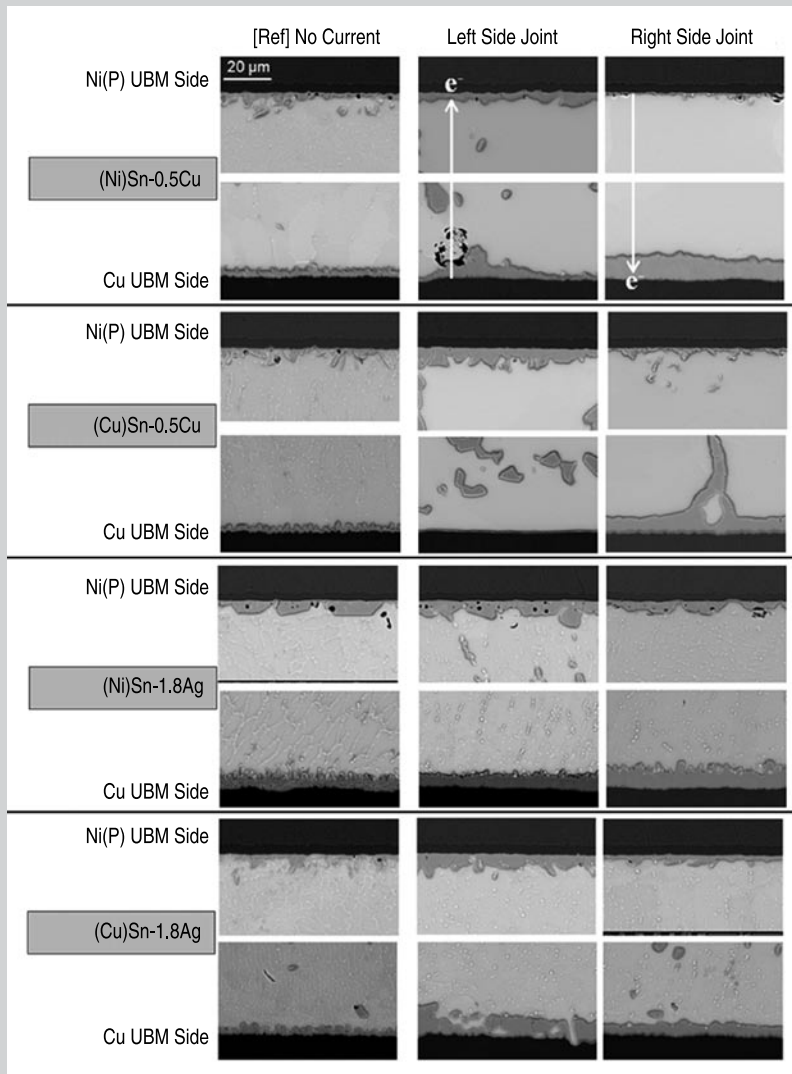


Figure 7. Interfacial IMC layers of four solder joints under no current stressing and under 14k A/cm² constant current stressing for 10 h.

This is expected because much of Cu atoms move fast together with the electron flow through many high-angle grain boundaries observed in Sn-0.5Cu joints. In (Ni)Sn-1.8Ag joints, the consumption of UBMs and the thickness change of Cu₆Sn₅ layers at the left and right side joints are less than in Sn-0.5Cu joints. The initially thick IMC layers in (Ni)Sn-1.8Ag joints could serve as a barrier to prevent the dissolution of Cu or Ni from either UBM into solder. However, in (Cu)Sn-1.8Ag joints, the thickness change of Cu₆Sn₅ layers at both interfaces of the left-side joint is larger than in (Ni)Sn-1.8Ag joints, resulting in a thicker IMC layer. Overall, 60° twin boundary of (Cu)Sn-1.8Ag joints and initial thin IMC layers seem to facilitate fast Cu migration from the cathode to the anode side.

In summary, the stable microstructure having low-angle large grains with near <100> or <110> or <111> orientations, the stable IMC particles such as Ag₃Sn, and the thick IMC layers in as-reflowed joints are the contributing factors for better EM performance of Sn-rich solder joints.

CONCLUSIONS

In this study, the electromigration performance of Pb-free solder joints is investigated in terms of solder com-

position (Sn-0.5Cu and Sn-1.8Ag) and joining path to Cu or Ni(P) UBM. The important findings are summarized as follows.

1. Solder composition (Sn-0.5Cu vs. Sn-1.8Ag) and joining path to Cu or Ni(P) UBM significantly affect the grain orientation of β -Sn and IMC layers at the UBM interfaces, which in turn influence the EM lifetime of Sn-rich solder joints.
2. Under 9,900 A/cm² and 14,150 A/cm² current stressing, the MTTF ranking of solder joints, from the worst to best, is (Cu)Sn-0.5Cu \cong (Ni)Sn-0.5Cu < (Cu)Sn-1.8Ag << (Ni)Sn-1.8Ag.
3. In (Cu)Sn-0.5Cu and (Ni)Sn-0.5Cu joints, Cu atoms move together with electron flow fast through high-angle grain boundaries under current stressing. Fast migration of Cu and Ni atoms damage UBM layers and reduce the lifetime of solder joints.
4. In (Cu)Sn-1.8Ag joints, Cu atoms migrate fast through 60° twin boundary under current stressing. However, since Ag atoms hardly migrate to the anode side under current stressing, Sn-1.8Ag joints

have a longer EM lifetime than Sn-0.5Cu joints.

5. In (Ni)Sn-1.8Ag joints, because of their stable microstructure of low-angle large grains combined with stable Ag₃Sn particles, Cu atoms move slowly through low-angle grain boundaries and Sn lattice under current stressing. In addition, the initial thick IMC layers at both interfaces would retard UBM dissolution and enhance EM lifetime.

ACKNOWLEDGEMENTS

This work was supported by grant no. EEWS-2010-N01100048 from EEWS Research Project of the office of KAIST EEWS Initiative. (EEWS: Energy, Environment, Water, and Sustainability) We also appreciate the support of Dr. Young-Boo Lee and Seong-Hwan Cho at the Korea Basic Science Institute (KBSI) for assistance with the EPMA analysis.

References

1. K.N. Tu et al., *AIP Conference Proceedings*, 817 (2006), pp. 327–338.
2. L. Nicholls et al., *Proc. 59th Electronic Components and Technology Conf.* (Piscataway NJ: IEEE, 2009), pp. 914–921.

3. P. Su and L. Li, *Proc. 59th Electronic Components and Technology Conf.* (Piscataway NJ: IEEE, 2009), pp. 903–908.
4. S.W. Liang et al., *J. Electron. Mater.*, 38 (2009), p. 2443.
5. W.K. Choi, S.W. Yoon, and H.M. Lee, *Mater. Trans.*, 42 (2001), p. 783.
6. S.-K. Seo et al., *J. Electron. Mater.*, 35 (2006), p. 1975.
7. D.H. Kim et al., *J. Electron. Mater.*, 38 (2009), p. 39.
8. M.G. Cho et al., *J. Electron. Mater.*, 36 (2007), p. 1501.
9. B.F. Dyson, *J. Appl. Phys.*, 37 (1966), p. 2375.
10. B.F. Dyson, T.R. Anthony, and D. Turnbull, *J. Appl. Phys.*, 37 (1967), p. 3408.
11. D.C. Yeh and H.B. Huntington, *Phys. Rev. Lett.*, 53 (15) (1984), p. 1469.
12. F.H. Huang and H.B. Huntington, *Phys. Rev. B*, 9 (4) (1974), p. 1479.
13. M. Lu et al., *Appl. Phys. Lett.*, 92 (2008), 211909.
14. S.-K. Seo et al., *J. Electron. Mater.*, 38 (2009), p. 2461.
15. S.-K. Seo et al., *J. Electron. Mater.*, 38 (2009), p. 257.
16. G.F. Bolling, J.J. Kramer, and W.A. Tiller, *Trans. Met. Soc. AIME*, 227 (1963), p. 1453.
17. S.-K. Seo, M.G. Cho, and H.M. Lee, *J. Mater. Res.* (under review).
18. C.E. Ho, S.C. Yang, and C.R. Kao, *J. Mater. Sci: Mater. Electron.*, 18, (2007), p. 155.

Sun-Kyoung Seo and Moon Gi Cho are senior engineers with Samsung Electronics, Yongin, Republic of Korea; Sung K. Kang, research staff member, is with the IBM T.J. Watson Research Center, Yorktown Heights, New York 10598, USA; and Hyuck Mo Lee, professor, is with the Department of Materials Science and Engineering, KAIST, 335 Gwahangno, Yuseong-gu, Daejeon 305-701, Republic of Korea. Dr. Lee can be reached at hmlee@kaist.ac.kr.